arXiv:1202.5607v1 [quant-ph] 25 Feb 2012

Fraunhofer diffraction of Stokes photons from cold atomic ensembles: entanglement witness, and collectively enhanced metrology

Hongyi Yu and Wang Yao
Department of Physics and Center of Theoretical and Computational Physics,
The University of Hong Kong, Hong Kong, China

(Dated: February 28, 2012)

Diffraction refers to the interference phenomena of propagating wave when encountering scatters, and has been a powerful tool for revealing the geometry. Inelastically scattered photons also carry phase information from internal degrees of freedom such as spin of the scatter,[1–9] a new ingredient for diffraction phenomena. Here we exploit the Fraunhofer diffraction of Stokes photons for detecting spin entanglement and for probing spin and motional dynamics in cold atomic ensembles. For many-body states where the spin-excitation number has small or maximum uncertainty, entanglement is witnessed by a qualitative diffraction feature, namely a sharp peak or dip in a chosen direction. For general states, the spin pair-correlation sum can be read out from the relative strength of the peak or dip over its background which, together with the expectation value and uncertainty of spin-excitation number, detect entanglement through the spin squeezing inequalities.[10–13] Spin precessions in Zeeman field gradient lead to displacement of the diffraction peak or dip while atomic motions lead to decay of its strength. These can serve as principles for vector gradiometer of fields and for non-demolition measurement of atomic temperature and collisional dynamics. Using a spin-coherent-state of N unentangled atoms as the probe, the information of interest are encoded by a collectively-enhanced diffraction peak of strength $\sim N^2$, making possible gradiometer with $1/N$ sensitivity and thermometer by a single shot.

For atoms in a Λ configuration, two hyperfine ground states can be coupled to a common excited state by optical fields of different frequencies. With one of the transitions coupled by a laser, a spin-excitation in the ground state manifold can be converted into a Stokes photon through a spontaneous Raman transition with phase information preserved. This process has been extensively explored as an interface between flying single photons and quantum memory based on collective spin-excitations in atomic ensembles.[1–9] With a detuned laser, the conversion of collective spin-excitations to Stokes photons has the same description to the collective spontaneous emission by excited two-level atoms.[14] The latter has been another topic of fundamental interest especially in connection with the phenomenon of super-radiance from very dense ensembles where atoms are close together compared to the optical wavelength.[15–17] Recent studies have extended this phenomenon to a new paradigm, namely the single photon super-radiance by atomic ensembles prepared with single collective excitation.[14,18–21]

Here we exploit a sharp feature in the Fraunhofer diffraction of Stokes photons for detecting spin entanglement and for probing spin and motional dynamics in cold atomic ensembles, where interatomic distance is typically comparable to or larger than the optical wavelength. We show the sum of spin pair-correlations in a general many-body state can be read out from the relative strength of a sharp diffraction peak or dip over its background (Fig. 1). This pair-correlation sum together with the expectation value and uncertainty of spin-excitation number are sufficient for detecting entanglement through available spin squeezing inequalities,[12,13] expressed as pair-correlation sum rules. In the limit of small uncertainty of spin-excitation number entanglement is verified simply by seeing either a diffraction peak or dip, while in the opposite limit of maximum uncertainty entanglement is verified by seeing a dip. Conserved by atomic collisions, the pair-correlation sum only decays in a slow timescale equal to the single spin dephasing time, hence this entanglement detection is robust and applicable for cold atom gas as well as atoms in optical lattices. In ensembles with many spin-excitations, the large photon counts from each individual measurement cycle can greatly facilitate the detection. Entanglement between excited two-level atoms can be detected in the same way from the angular distribution of spontaneously emitted photons.

Inhomogeneous spin precessions in a Zeeman field gradient lead to displacement of the diffraction peak (dip) preserving its shape and relative strength. This makes possible calibration of inhomogeneity in optical lattices with a precision limited only by the single spin homogeneous broadening. It is also a principle for ultra-sensitive vector gradiometer of fields. The gradient is simultaneously measured by the $\sim N^2$ pair-correlations of a N-body wavefunction. Using a spin-coherent-state as the probe state, the gradient is encoded as the displacement of a diffraction peak of strength $\sim N^2$, an analog of the multi-slit interferometry. As a result, the gradiometer sensitivity has the $1/N$ scaling, an example of collectively enhanced metrology without entanglement.[22–26] In trapped atomic gases, motional dynamics results in temporal decay of the peak which can be used for non-demolition probe of temperature and collisional interactions.

Consider an optically thin cold atomic ensemble driven by a detuned laser with wavevector $\mathbf{k}_0 = k_0\hat{\mathbf{z}}$, and atomic motion can be considered as frozen in the duration of photon emission. Emission of a Stokes pho-

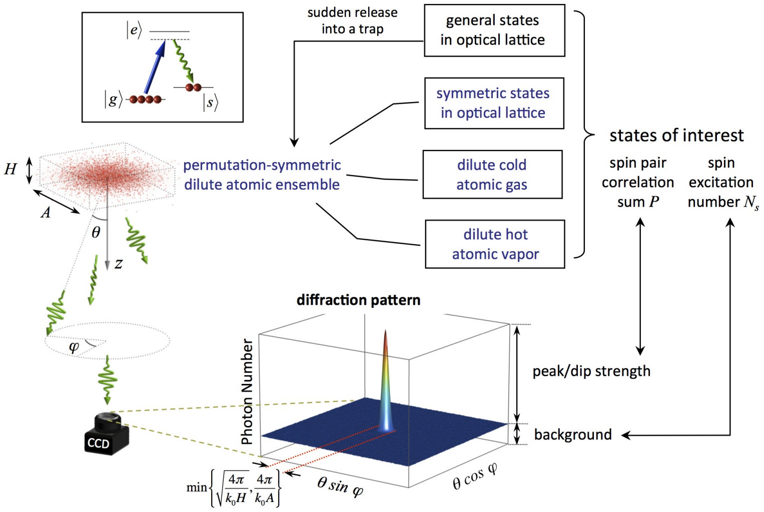
$|e\rangle$
$|g\rangle$
$|s\rangle$
sudden release into a trap
general states in optical lattice
symmetric states in optical lattice
dilute cold atomic gas
dilute hot atomic vapor
states of interest
spin pair correlation sum P
spin excitation number N_s
H
A
permutation-symmetric dilute atomic ensemble
θ
z
φ
CCD
diffraction pattern
Photon Number
peak/dip strength
background
$\min\left\{\sqrt{\frac{4\pi}{k_0 H}}, \frac{4\pi}{k_0 A}\right\}$
$\theta \sin \varphi$
$\theta \cos \varphi$

FIG. 1: **Fraunhofer diffraction of Stokes photons from permutation-symmetric dilute ensembles**. Atoms are driven by a detuned laser with wavevector $\mathbf{k}_0 = k_0\hat{\mathbf{z}}$. The pair-correlation sum P in the many-atom state of interest manifests as a sharp diffraction peak (for positive P) or dip (for negative P) along the forward direction, with a width inversely proportional to the ensemble size. The value of P can be read out from the relative strength of the peak or dip to its background, provided that photon emission is either much faster (for cold atoms) or much slower (for hot atomic vapor) than atomic motions. This diffraction feature can be measured in a chosen direction with finite θ to avoid laser photons when a Zeeman field gradient imprints a phase gradient on the initially permutation-symmetric ensemble (cf. Fig .3).

ton into mode $\mathbf{k} = (k, \theta, \varphi)$ where $k \cong k_0$ is accompanied by the annihilation of a spin excitation by $\hat{J}^-(\Delta\mathbf{k}) \equiv \sum_{j=1}^{N} \mathrm{e}^{-i\Delta\mathbf{k}\cdot\mathbf{r}_j}\hat{\sigma}_j^-$, $\Delta\mathbf{k} = \mathbf{k} - \mathbf{k}_0$. The angular distribution of the photon emission rate is given by $I(\theta,\varphi,t) = I_s(\theta)I_c(\theta,\varphi,t)$. I_s is the single atom dipole emission pattern, a slow varying function of θ. $I_c(\theta,\varphi,t) \equiv \mathrm{Tr}[\hat{J}^+(\Delta\mathbf{k})\hat{J}^-(\Delta\mathbf{k})\rho(t)]$ is the collective factor where $\rho(t)$ is the atomic density matrix. At the initial time of photon emission,

$$\begin{aligned} I_c(\theta,\varphi,0) &= \langle \hat{N}_s\rangle + \sum_{j\neq j'} \mathrm{e}^{-i\Delta\mathbf{k}\cdot(\mathbf{r}_j - \mathbf{r}_{j'})}\langle\hat{\sigma}_{j'}^+\hat{\sigma}_j^-\rangle \qquad (1) \\ &= \langle \hat{N}_s\rangle - \frac{P}{N-1} + P\frac{|\langle\sum_j e^{-i\Delta\mathbf{k}\cdot\mathbf{r}_j}\rangle|^2}{N^2-N}, \end{aligned}$$

where $\hat{N}_s \equiv \sum_j(\hat{\sigma}_j^z + 1)/2$ is the spin-excitation number operator. Here and hereafter $\langle\cdots\rangle$ denotes the expectation value over $\rho(0)$, the many-body state of interest. $P \equiv \langle\sum_{j\neq j'}\hat{\sigma}_{j'}^+\hat{\sigma}_j^-\rangle$ is thus the sum of spin pair-correlations. The last equal sign in Eq. (1) holds when $\rho(0)$ is invariant under permutation of atoms, which is the typical situation for atom gases. For general states in optical lattices, by sudden release of atoms into a spin-independent trap,[27] the density matrix averaged over many ensemble copies will become permutation-symmetric after atoms lose memory of their initial positions, with P preserved. $|\langle\sum_j e^{-i\Delta\mathbf{k}\cdot\mathbf{r}_j}\rangle|^2$ is a sharp feature which equals to N^2 along the forward direction ($\theta = 0$), and vastly drops to zero for $\theta \geq \theta_b \equiv \min\{\sqrt{\frac{\pi}{k_0 H}}, \frac{2\pi}{k_0 A}\}$ where A and H are respectively the transverse and longitudinal size of the ensemble (Fig. 1). Thus, positive (negative) pair-correlation sum manifests as a sharp diffraction peak (dip), and P can be read out from the ratio of the peak (dip) to the background: $\frac{I(\theta=0)-I(\theta_b)}{I(\theta_b)} = \frac{P}{\langle\hat{N}_s\rangle - P/N}$.

With the spin-excitation number conserved in many physical processes, its expectation value $\langle\hat{N}_s\rangle$ and uncertainty $\Delta N_s \equiv \sqrt{\langle\hat{N}_s^2\rangle - \langle\hat{N}_s\rangle^2}$ are usually known a priori. The peak (dip) to background ratio is then sufficient to detect entanglement via available spin squeezing inequalities derived for first and second moments of total spin.[10–13] The longitudinal component of total spin is equivalent to the spin-excitation number: $\hat{J}_z = \hat{N}_s - N/2$, and the second moment of transverse components is equivalent to the pair-correlation sum: $\langle\hat{J}_x^2\rangle + \langle\hat{J}_y^2\rangle = P + N/2$. Many spin squeezing inequalities can thus be formulated as pair-correlation sum rules. For example, the optimal spin squeezing inequalities discovered in Ref. 12 become:

$$\begin{aligned} P &\leq (N-1)\Delta N_s^2, &\text{(2a)} \\ P &\geq -\Delta N_s^2, &\text{(2b)} \\ (N-1)P &\geq \langle\hat{N}_s^2\rangle - N\langle\hat{N}_s\rangle. &\text{(2c)} \end{aligned}$$

Violation of any one of Eq. (2a-2c) implies entanglement.

Entanglement detection based on the above pair-correlation sum rules is described by the phase diagrams shown in Fig. 2(a-c). For eigenstates of $\hat{J}^2$ and $\hat{J}_z$, the phase space characterized by the total spin quantum number J and the magnetic quantum number M consists of two continuous regions corresponding to diffraction peak and dip in the forward direction, respectively.

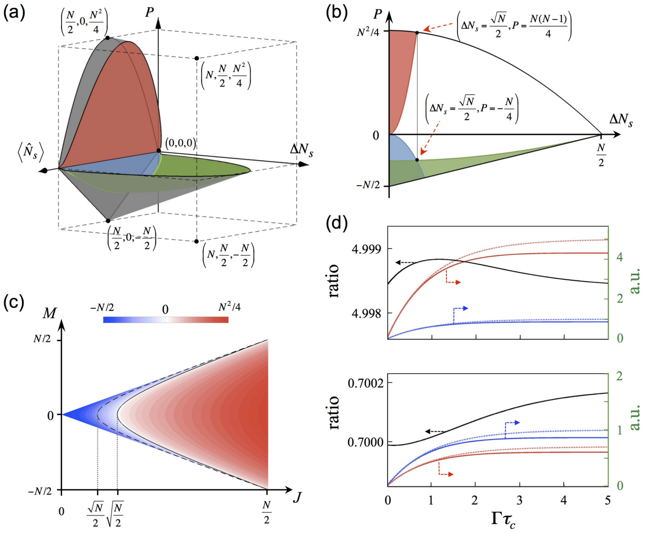

FIG. 2: **Entanglement detection from the diffraction peak or dip**. (a) Phase diagram in the parameter space $(\langle\hat{N}_s\rangle, \Delta N_s, P)$, being respectively the expectation value and uncertainty of the spin-excitation number, and the pair-correlation sum. States in the surrounded region are all entangled ones. (b) A slice of the diagram in (a) taken for half-spin-excitation states, i.e. $\langle\hat{N}_s\rangle = N/2$. The red, blue and green regions are entangled states violating inequalities Eq. (2a), (2b) and (2c) respectively. The grey surfaces in (a) and the black curves in (b) are boundaries between physical and unphysical regions. Positive and negative sections of P axis have different linear scale. (c) Strength of the diffraction peak or dip for eigenstates of total spin $\hat{J}^2$ and $\hat{J}_z$. This phase space consists of a peak region and a dip region, violating Eq. (2a) and (2b) respectively. States violating Eq. (2c) are to the left of the dashed curve. (d) Upper (lower): peak (dip) to background ratio as a function of the collection interval τ_c for a half-spin-excitation state with $P = 2.5N$ $(P = -0.35N)$, shown as the black curve. The calculation is for $N = 4000$ atoms of a 2D Gaussian distribution with FWHM $A = 100$ μm. Peak or dip (background) strength is evaluated at $\theta = 0$ $(\theta = \frac{2\pi}{k_0 A})$, shown by the blue (red) solid curve. Dashed curves are calculations with the multiple-light scattering and dipole-dipole interaction neglected.

States in the peak (dip) region are all entangled ones violating Eq. (2a) (Eq. (2b)). States violating Eq. (2c) form a subset of the dip region. For a general many-body state, the diffraction pattern is simply the weighted average of these patterns associated with definite J and M, since $\sum_{j\neq j'} \hat{\sigma}_j^+ \hat{\sigma}_{j'}^-$ does not mix states of different J and M. *Qualitative* criteria become possible for entanglement witness in two limits. With vanishing ΔN_s seeing either a sharp diffraction peak or dip verifies entanglement, while with maximum ΔN_s seeing a dip verifies entanglement (Fig. 2(a-b)). On the other hand, a peak (dip) strength exceeding some threshold value always implies entanglement. Taking half-spin-excitation states for example, observing a dip to background ratio $|r| \geq \frac{1}{2}$ or a peak to background ratio $r \geq \frac{N(N-1)}{N+1}$ verifies entanglement for any possible ΔN_s. Moreover, P and ΔN_s can also quantify the entanglement depth in the vicinity of Dicke states.[13]

Through these pair-correlation sum rules, the initial diffraction pattern detects entanglement in non-condensed atomic ensemble regardless of shape and density. Hereafter, we focus on dilute ensembles where interatomic distance is comparable to or larger than optical wavelength. Remarkably, under this condition, one can collect all Stokes photons, not only those initial ones, for measuring the pair-correlation sum in $\rho(0)$. The diffraction pattern at an arbitrary time is determined by the instantaneous atomic density matrix $\rho(t)$ which defers from $\rho(0)$ with spin-excitations annihilated. Nevertheless, in dilute ensembles, the evolution of ρ under the spontaneous Stokes scattering is dominated by independent decay of spins which preserves the initial diffraction pattern (see methods section). Corrections from the multiple-light scattering and dipole-dipole interaction, which need nonperturbative treatment in the dense limit,[15,16] are well accounted here by perturbation theory. We find these weak processes only result in slow varying modulation of the diffraction pattern, barely changing the ratio of the sharp peak or dip to its neighboring background. Namely,

$$r(\tau_c) \equiv \frac{n(\theta=0,\tau_c) - n(\theta_b,\tau_c)}{n(\theta_b,\tau_c)} \cong \frac{P}{\langle\hat{N}_s\rangle - P/N} \qquad (3)$$

where $n(\theta,\varphi,\tau_c) \equiv \delta\Omega \int_0^{\tau_c} dt I(\theta,\varphi,t)$ is the number of photons emitted into an infinitesimal solid angle in the collection interval $0 \leq t \leq \tau_c$. For a dilute ensemble Eq. (3) holds for arbitrarily large τ_c (cf. Fig. 2(d)). This is greatly helpful in ensembles with large $\langle\hat{N}_s\rangle$, since large number of photons can be collected in each measurement cycle to facilitate the entanglement detection.

We estimate the range of applicability of our treatment. The dilute condition is satisfied by typical cold atom gases of a density $10^{10} - 10^{12}$ cm^{-3} or by atoms in optical lattice. The duration of Stokes photon emission is of a timescale $\Gamma^{-1} = (\frac{\Omega_L}{2\Delta})^{-2}\Gamma_0^{-1}$, where Ω_L is the laser Rabi frequency and Δ the detuning. The excited state decay rate $\Gamma_0 \gtrsim 30$ μs^{-1} for typical alkali atoms.[28] Taking $(\frac{\Omega_L}{2\Delta})^{-2} \sim 40$, all Stokes photons are emitted in a timescale $\Gamma^{-1} \lesssim$ μs. For cold atom gases with a temperature of $1-100$ μK, the average velocity is $0.01-0.1$ m/s. Hence atoms can only travel $10-100$ nm in the duration of Γ^{-1} which is negligible as compared to the light wavelength. Moreover, we find that pair-correlation sum of a dilute hot atomic vapor can be measured in the same way if Stokes photon emission is controlled to be much slower than atomic motions (see supplementary material).

Under free evolution, the pair-correlation changes as $\mathrm{Tr}[\hat{\sigma}_{i'}^+ \hat{\sigma}_i^- \rho(\tau)] = e^{i(\eta_i t_0 - \eta_{i'}\tau) - 2\gamma\tau} \mathrm{Tr}[\hat{\sigma}_{i'}^+ \hat{\sigma}_i^- \rho(0)]$, where η_i is the Zeeman frequency and γ the homogeneous dephasing rate of an individual spin. The pair-correlation sum thus decays only at the single spin dephasing rate. Therefore entanglement in $\rho(0)$ can be reliably detected from

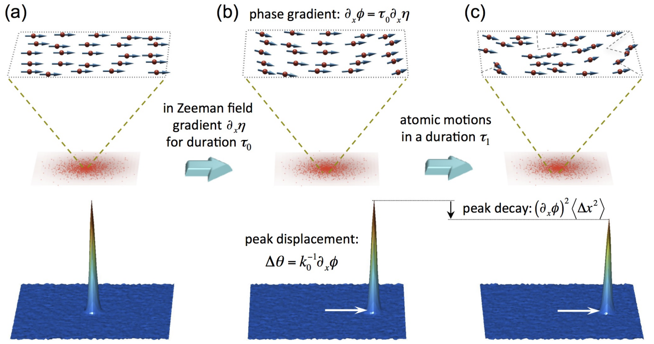
(a)
(b)
phase gradient: $\partial_x\phi = \tau_0\partial_x\eta$
(c)
in Zeeman field gradient $\partial_x\eta$ for duration τ_0
atomic motions in a duration τ_1
peak decay: $(\partial_x\phi)^2\langle\Delta x^2\rangle$
peak displacement: $\Delta\theta = k_0^{-1}\partial_x\phi$

FIG. 3: **Diffraction patterns (lower parts) from atomic ensemble in different spin configurations (upper).** (a) Spin-coherent-state with in-plane polarization. (b) Evolution in a Zeeman field gradient imprints a phase gradient of spins, resulting in a displacement of the diffraction peak which can be a principle of gradiometer. (c) Atomic motions diminish the spin polarization, resulting in decay of the displaced peak. This can be a principle for non-demolition measurement of atomic temperature and collisional interactions.

the dephased state $\rho(\tau)$ as long as $\tau \ll \gamma^{-1}$, even when the fidelity is exponentially small with N.[13]

Spatial inhomogeneity of external fields leads to position dependent Zeeman frequency $\eta(\mathbf{r})$ and hence inhomogeneous precessions of spins. If the size of the ensemble is small compared to the variation length scale of the field, the dominating term is the gradient: $\eta(\mathbf{r}) \cong \mathbf{r}\cdot\nabla\eta$. For an ensemble initially in a permutation-symmetric state, after an interval τ_0 with frozen motion in the Zeeman field gradient, the diffraction pattern becomes $I_c = \langle\hat{N}_s\rangle - \frac{P}{N-1} + \frac{P}{N^2-N}|\langle\sum_j e^{-i(\Delta\mathbf{k}-\tau_0\nabla\eta)\cdot\mathbf{r}_j}\rangle|^2$. We focus on situations where $\partial_z\eta$ is either zero or not picked up by atomic ensembles of a quasi-2D geometry in $x-y$ plane. The in-plane gradient simply results in a displacement of the sharp diffraction peak or dip, preserving its strength and shape (Fig. 3). This has several significant consequences. First, by evolution in an external field of known gradient, entanglement can be detected by measuring the peak or dip along a chosen direction with finite θ, such that detectors do not pick up laser photons. Second, the displacement measures the vector value of unknown gradient. This can be used to calibrate inhomogeneous broadening in optical lattices. The Zeeman field gradient can come from the gradient of magnetic field, static electric field via dc Stark effect, and light field via ac Stark effect.[8] The physics discussed here can thus be used as a principle of vector gradiometer of these fields with a spatial resolution equal to the ensemble size A.

An ideal probe state is simply the spin-coherent-state of N unentangled atoms with in-plane polarization. The gradient is then probed simultaneously by the $\sim N^2$ classical pair-correlations, and its vector value is encoded as the displacement of a diffraction peak with strength $\sim N^2$. This N^2 scaling of the peak strength suggests an enhancement of the sensitivity by using large group of atoms collectively, as compared to uncorrelated probes using small groups. In a 1D geometry (Fig. 4), a single collective probe using N atoms can achieve a sensitivity of $\sim \frac{1}{N}\frac{k_0}{\tau_0\sqrt{k_0 A}}$, which goes beyond the standard quantum limit of $\sim \frac{1}{\sqrt{N}}\frac{k_0}{\tau_0\sqrt{k_0 A}}$ for $N/2$ independent probes using atom-pairs. This collectively-enhanced sensitivity with $1/N$ scaling is valid in the dilute regime $N \leq k_0 A$. Beyond this regime, the multiple light scattering can not be treated perturbatively and its effect will eventually renormalize the peak strength to the N scaling. By trapping atoms in optical lattices, the probe time τ_0 can be as long as the single spin homogeneous dephasing time, in the order of second or longer.[8] This diffraction based gradiometer using stationary atoms is immune to collective noises and uncertainty in atomic positions. In comparison, the gradiometer based on Mach-Zehnder interferom-

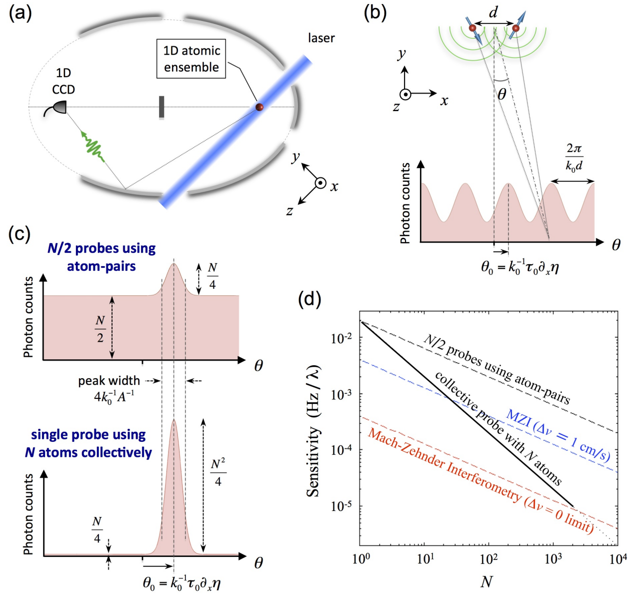

FIG. 4: **Zeeman field gradiometer using a 1D atomic ensemble.** (a) and (b) Schematic of the setup. The ensemble and a 1D CCD array are placed respectively on the two common focus lines of a group of elliptical cylinder mirrors. The smallest ensemble can be an atom-pair, giving a direct analog of the double-slit interferometry. (c) Signal of $N/2$ probes using atom-pairs (upper), and single probe using N atoms collectively (lower), with each atom placed randomly on the focus line according to a Gaussian distribution with FWHM A. The peak strength of the lower is enhanced by a factor of N. (d) Gradiometer sensitivity at a spatial resolution $A = 1$ mm with a resource of N unentangled atoms. The diffraction based gradiometer using N atoms collectively ($N/2$ atom-pairs independently) has a sensitivity of the $1/N$ ($1/\sqrt{N}$) scaling, shown by the solid (dashed) black line. Sensitivity of flying atom Mach-Zehnder interferometry (MZI) gradiometer is shown for reference.[29] The probe time $\tau_0 = \frac{A}{\Delta v} = 0.1$ s for the blue line, limited by a finite velocity uncertainty $\Delta v = 1$ cm/s, while $\tau_0 = 1$ s for all other lines, limited only by the single spin dephasing time.

etry of flying atoms in atomic fountain has the standard quantum limited sensitivity of $\sim \frac{1}{\sqrt{N}}\frac{1}{\tau_0 A}$,[29,30] but the inevitable velocity uncertainty sets a tighter upper bound for τ_0 dependant on the spatial resolution A (see section VD in supplementary material).

Finally, we present a principle for non-demolition probe of atomic motions and temperature in trapped cold atom gases (see Fig. 3). A phase gradient $\nabla\phi$ is first imprinted on the spin-coherent-state.[8] After a waiting time τ_1, we turn on the laser and measure the diffraction pattern of Stokes photons. Atomic motions in the interval τ_1 will diminish the spin polarization, resulting in decay of the displaced diffraction peak.[7] For $|\nabla\phi|^2\langle\Delta\mathbf{r}^2\rangle \ll 1$, the peak strength is $\frac{N^2}{4}e^{-|\nabla\phi|^2\langle\Delta\mathbf{r}^2\rangle/3}$, $\langle\Delta\mathbf{r}^2\rangle$ being the mean square displacement of atoms. For short τ_1 when $\Delta\mathbf{r}$ is small compared to the interatomic distance d, $\langle\Delta\mathbf{r}^2\rangle = 2\frac{k_BT}{m}\tau_1^2$. Thus, by preparing a large phase gradient $|\nabla\phi| \sim \frac{1}{d}$, this short time motion of atoms can be probed and the atomic temperature can be read out from the decay of the peak. Smaller $|\nabla\phi|$ allows the probe of long time motion which will eventually crossover to the diffusive regime by atom collisions. τ_1 is upper limited by the spin dephasing time, which is long enough for observing the entire crossover behavior from ballistic to diffusive motions, providing information about the collisional interactions in trapped cold atom gases. The collectively enhanced peak strength of $\sim N^2$ provides sufficient signal-to-noise ratio for determining $\langle\Delta\mathbf{r}^2\rangle$ at a given τ_1 by a single shot measurement.

Methods

Light-atom interaction. Consider atoms of a Λ level configuration where two atomic ground states $|g\rangle$ and $|s\rangle$ can be optically coupled to a common excited state $|e\rangle$ (Fig. 1 inset). With a coherent laser of Rabi frequency Ω_L, detuning Δ, and wavevector $\mathbf{k}_0 = k_0\hat{\mathbf{z}}$ coupling the $|s\rangle$ to $|e\rangle$ transition, an atom can go from state $|s\rangle$ to $|g\rangle$ by emitting a Stokes photon into the vacuum. When Δ is much larger than Ω_L and the excited state homogeneous line width Γ_0, $|e\rangle$ can be adiabatically eliminated, leading to the effective light-atom coupling in the electric-dipole and rotating wave approximation:

$$\begin{aligned}\hat{H} &= \sum_{\mathbf{k}}\hbar\omega_k\hat{a}^\dagger_{\mathbf{k}}\hat{a}_{\mathbf{k}} + \sum_j \bar{E}_z\hat{\sigma}^z_j \\ &\quad + \sum_{\mathbf{k}} g_{\mathbf{k}}\sum_j \mathrm{e}^{-i(\mathbf{k}-\mathbf{k}_0)\cdot\mathbf{r}_j}\hat{\sigma}^-_j\hat{a}^\dagger_{\mathbf{k}} + \text{h.c.},\end{aligned}$$

where $g_{\mathbf{k}} = \frac{\Omega_L}{2\Delta}\sqrt{\frac{2\pi\omega_k}{V}}\hat{\mathbf{e}}_{\mathbf{k}}\cdot\boldsymbol{\mu}$, $\hat{\mathbf{e}}_{\mathbf{k}}$ and $\boldsymbol{\mu}$ being respectively the unit polarization vector and the single atom dipole. The ac Stark shift has been grouped into $\bar{E}_z$, and the pseudospin operators are defined in the ground state manifold: $\hat{\sigma}^-_j \equiv |g\rangle_j\langle s|$ and $\hat{\sigma}^z_j \equiv |s\rangle_j\langle s| - |g\rangle_j\langle g|$. We assume anti-Stokes scattering is either forbidden by the polarization selection rule or suppressed by the much larger detuning when $\bar{E}_z \gg \Delta$.

The same Hamiltonian can also describe spontaneous emission of excited two-level atoms where the excited state $|e\rangle$ decays to ground state $|g\rangle$ by emitting a photon into the vacuum. In such case, $g_{\mathbf{k}} = \sqrt{\frac{2\pi\omega_k}{V}}\hat{\mathbf{e}}_{\mathbf{k}}\cdot\boldsymbol{\mu}$ and the pseudospin operators $\hat{\sigma}^-_j \equiv e^{-i\mathbf{k}_0\cdot\mathbf{r}_j}|g\rangle_j\langle e|$ and $\hat{\sigma}^z_j \equiv |e\rangle_j\langle e| - |g\rangle_j\langle g|$ are defined for the j-th atom located at $\mathbf{r}_j$.

Perturbative solution of master equation. Under the above light-atom interaction, the evolution of the atomic density matrix is described by the Lindblad master equation in the Born-Markov approximation:

$$\begin{aligned}\frac{d\rho}{dt} &= \mathcal{L}_0\rho(t) + \mathcal{L}_1\rho(t) \\ \mathcal{L}_0\rho(t) &\equiv \sum_j \frac{\Gamma}{2}\left(2\hat{\sigma}^-_j\rho\hat{\sigma}^+_j - \hat{\sigma}^+_j\hat{\sigma}^-_j\rho - \rho\hat{\sigma}^+_j\hat{\sigma}^-_j\right) \\ \mathcal{L}_1\rho(t) &\equiv \sum_{j\neq j'}\frac{\Gamma_{jj'} - iG_{jj'}}{2}(\hat{\sigma}^-_j\rho\hat{\sigma}^+_{j'} - \hat{\sigma}^+_{j'}\hat{\sigma}^-_j\rho) + h.c.,\end{aligned}$$

where $\Gamma_{jj'} = \Gamma\frac{\sin(k_0|\mathbf{r}_j-\mathbf{r}_{j'}|)}{k_0|\mathbf{r}_j-\mathbf{r}_{j'}|}$ and $G_{jj'} = \Gamma\frac{\cos(k_0|\mathbf{r}_j-\mathbf{r}_{j'}|)}{k_0|\mathbf{r}_j-\mathbf{r}_{j'}|}$ describe respectively the multiple light scattering and dipole-dipole interaction.[14,17] In the study of superradiance phenomena in very dense atomic ensembles, these effects must be accounted non-perturbatively.[15] $\Gamma_{jj'}$ and $G_{jj'}$ drop fast with distance. In dilute atomic ensembles where the atom-atom distance is comparable or larger than the photon wavelength, the atomic evolution can be solved perturbatively. Using the Laplace transform $w(z) = \int_0^\infty dt\mathrm{e}^{-zt}\rho(t)$, we have

$$w(z) = \frac{1}{z - \mathcal{L}_0 - \mathcal{L}_1}\rho(0).$$

For $k_0|\mathbf{r}_j - \mathbf{r}_{j'}| \geq 2\pi$, $\mathcal{L}_1$ is small compared to $\mathcal{L}_0$, and we make a perturbative expansion $\frac{1}{z-\mathcal{L}_0-\mathcal{L}_1} = \frac{1}{z-\mathcal{L}_0} + \frac{1}{z-\mathcal{L}_0}\mathcal{L}_1\frac{1}{z-\mathcal{L}_0} + \cdots$. By inverse Laplace transform we can get the solution of the atomic density matrix $\rho^{(n)}$ keeping up to the n-th order effects of $\mathcal{L}_1$.

For the zeroth order solution $\rho^{(0)}(t) = \mathrm{e}^{\mathcal{L}_0 t}\rho(0)$, we find $\mathrm{Tr}[\hat{J}^+(\mathbf{k})\hat{J}^-(\mathbf{k})\rho^{(0)}(t)] = e^{-\Gamma t}\mathrm{Tr}[\hat{J}^+(\mathbf{k})\hat{J}^-(\mathbf{k})\rho(0)]$, i.e. the initial diffraction pattern is preserved for all time. Comparisons with exact solution of master equation for a chain of 12 atoms show that the perturbation expansion converges fast for $k_0|\mathbf{r}_j - \mathbf{r}_{j'}| \geq 2\pi$, and the effects of the multiple light scattering and dipole-dipole interaction are well accounted by keeping only the first order effects of the $\mathcal{L}_1$ term:

$$\rho^{(1)}(t) = \rho^{(0)}(t) + \int_0^t d\tau\mathrm{e}^{\mathcal{L}_0\tau}\left[\mathcal{L}_1\rho^{(0)}(t-\tau)\right].$$

The $\mathcal{L}_1$ term leads to slow varying modulation of the diffraction pattern, which barely changes the ratio of the sharp peak (dip) to its neighboring background. Details on this modulation and the convergence check for the perturbative solutions can be found in the supplementary material.

---

[1] L.-M. Duan, M. D. Lukin, J. I. Cirac and P. Zoller, Long-distance quantum communication with atomic ensembles and linear optics, Nature **414**, 413 (2001).

[2] C. H. van der Wal, M. D. Eisaman, A. Andre, R. L. Walsworth, D. F. Phillips, A. S. Zibrov, and M. D. Lukin, Atomic Memory for Correlated Photon States, Science **301**, 196 (2003).

[3] B. Julsgaard, J. Sherson, J. I. Cirac, J. F. caronek, and E. S. Polzik, Experimental demonstration of quantum memory for light, Nature **432**, 482 (2004).

[4] D. N. Matsukevich, T. Chaneliere, S. D. Jenkins, S.-Y. Lan, T. A. B. Kennedy, and A. Kuzmich, Deterministic Single Photons via Conditional Quantum Evolution, Phys. Rev. Lett. **97**, 013601 (2006).

[5] J. Simon, H. Tanji, J. K. Thompson, and V. Vuletic, Interfacing Collective Atomic Excitations and Single Photons, Phys. Rev. Lett. **98**, 183601 (2007).

[6] C.-W. Chou, J. Laurat, H. Deng, K. S. Choi, H. de Riedmatten, D. Felinto, H. J. Kimble, Functional Quantum Nodes for Entanglement Distribution over Scalable Quantum Networks, Science **316**, 1316 (2007).

[7] B. Zhao, Y.-A. Chen, X.-H. Bao, T. Strassel, C.-S. Chuu, X.-M. Jin, J. Schmiedmayer, Z.-S. Yuan, S. Chen and J.-W. Pan, A millisecond quantum memory for scalable quantum networks, Nat. Phys. **5**, 95 (2009).

[8] U. Schnorrberger, J. D. Thompson, S. Trotzky, R. Pugatch, N. Davidson, S. Kuhr, and I. Bloch, Electromagnetically Induced Transparency and Light Storage in an Atomic Mott Insulator, Phys. Rev. Lett. **103**, 033003 (2009).

[9] R. Zhao, Y. O. Dudin, S. D. Jenkins, C. J. Campbell, D. N. Matsukevich, T. A. B. Kennedy, and A. Kuzmich, Long-lived quantum memory, Nat. Phys. **5**, 100 (2009).

[10] A. S. Sorensen and K. Molmer, Entanglement and Extreme Spin Squeezing, Phys. Rev. Lett. **86**, 4431 (2001).

[11] J. K. Korbicz, O. Guhne, M. Lewenstein, H. Haffner, C. F. Roos, and R. Blatt, Generalized spin-squeezing inequalities in N-qubit systems: Theory and experiment, Phys. Rev. A **74**, 052319 (2006).

[12] G. Tóth, C. Knapp, O. Gühne and H. J. Briegel, Optimal Spin Squeezing Inequalities Detect Bound Entanglement in Spin Models, Phys. Rev. Lett. **99**, 250405 (2007).

[13] L.-M. Duan, Entanglement Detection in the Vicinity of Arbitrary Dicke States, Phys. Rev. Lett. **107**, 180502 (2011).

[14] D. Porras and J. I. Cirac, Collective generation of quantum states of light by entangled atoms, Phys. Rev. A **78**, 053816 (2008).

[15] Rehler and Eberly, Superradiance, Phys. Rev. A **3**, 1735 (1971).

[16] M. Gross and S. Haroche, Superradiance: an essay on the theory of collective spontaneous emission, Phys. Rep. **93**, 301 (1982).

[17] J. P. Clemens, L. Horvath, B. C. Sanders, and H. J. Carmichael, Collective spontaneous emission from a line of atoms, Phys. Rev. A **68**, 023809 (2003).

[18] M. O. Scully, E. S. Fry, C. H. Raymond Ooi, and K. Wodkiewicz, Directed Spontaneous Emission from an Extended Ensemble of N Atoms: Timing Is Everything, Phys. Rev. Lett. 96, 010501 (2006)

[19] M. O. Scully and A. A. Svidzinsky, The Super of Superradiance, Science **325**, 1510 (2009).

[20] J. H. Eberly, Emission of one photon in an electric dipole transition of one among N atoms, J. Phys. B: At. Mol. Opt. Phys. **39**, S599 (2006).

[21] R. Wiegner, J. von Zanthier and G. S. Agarwal, Quantum-interference-initiated superradiant and subradiant emission from entangled atoms, Phys. Rev. A **84**, 023805 (2011).

[22] V. Giovannetti, S. Lloyd, and L. Maccone, Quantum-Enhanced Measurements: Beating the Standard Quantum Limit, Science **306**, 1330 (2004).

[23] M. J. Holland and K. Burnett, Interferometric Detection of Optical Phase Shifts at the Heisenberg Limit, Phys. Rev. Lett. **71**, 1355 (1993).

[24] J. Jacobson, G. Bjork, I. Chuang, and Y. Yamamoto, Photonic de Broglie Waves, Phys. Rev. Lett. **74**, 4835 (1995).

[25] B. L. Higgins, D. W. Berry, S. D. Bartlett, H. M. Wiseman and G. J. Pryde, Entanglement-free Heisenberg-limited phase estimation, Nature **450**, 393 (2007).

[26] D. Braun and J. Martin, Heisenberg-limited sensitivity with decoherence-enhanced measurements, Nature Communications **2**, 223 (2011).

[27] I. Bloch, J. Dalibard, and W. Zwerger, Many-body physics with ultracold gases, Rev. Mod. Phys. **80**, 885 (2008).

[28] L. J. Curtis, Precision Oscillator Strength and Lifetime Measurements, Springer Handbook of Atomic, Molecular, and Optical Physics, edited by W. F. Drake (Springer, 2005).

[29] M.-K. Zhou, Z.-K. Hu, X.-C. Duan, B.-L. Sun, J.-B. Zhao, and J. Luo, Precisely mapping the magnetic field gradient in vacuum with an atom interferometer, Phys. Rev. A **82**, 061602(R) (2010).

[30] J. B. Fixler, G. T. Foster, J. M. McGuirk and M. A. Kasevich, Atom Interferometer Measurement of the Newtonian Constant of Gravity, Science **315**, 74 (2007).

Acknowledgements

The authors thank X.D. Xu, S.W. Du, L.A. Wu, D.J. Wang, Q. Zhou and R.B. Liu for helpful discussions. The work was supported by the Research Grant Council of Hong Kong under Grant No. HKU706711P and HKU8/CRF/11G.